Piecewise smooth phase reconstruction

J. L. Marroquin

Centro de Investigación en Matemáticas, Apdo. Postal 402 Guanajuato, Guanajuato 36000, Mexico

J. A. Quiroga

Departamento de Optica, Facultad de Ciencias Físicas, Universidad Complutense de Madrid, Cuidad Universitaria s/n 28040, Madrid, Spain

R. Rodriguez-Vera

Centro de Investigaciones en Optica, Apdo. Postal 1-948 Leon, Guanajuato 37000, Mexico

Received August 16, 1999

A well-founded and computationally fast method is presented for filtering and interpolating noisy and discontinuous wrapped phase fields that preserves both the 2π discontinuities that come from the wrapping effect and the true discontinuities that may be present. It also permits the incorporation of an associated quality map, if it is available, in a natural way. Examples of its application to the computation of the isoclinic phase from photoelastic data and to the recovery of discontinuous phase fields from speckle interferometry are presented.

OCIS codes: 100.2000, 100.2650, 100.5070, 120.6160, 100.3020.

The reconstruction of phase maps from noisy data presents many problems, which include the presence of 2π discontinuities as a result of the wrapping that results from the arctangent computation, the possible presence of true discontinuities of the phase field, and the fact that the noise may have relatively low frequency components. However, in many cases it is possible to obtain a quality map that indicates whether the noisy phase map is reliable. What one would like is a filter that, first, could take into account this quality information when it is available and, second, could have an arbitrarily high filtering power but preserve the discontinuities that are present in the phase map. In this Letter we present an algorithm with these properties.

Suppose that one is given an observed phase field

$$\hat{\phi}_r = \arctan\left[\frac{I_s(r)}{I_c(r)}\right] \tag{1}$$

for $r \in L$, where L denotes the set of all pixels $r = (x, y)$ within the region of interest and I_s and I_c denote the sine and cosine (quadrature) observed images, respectively. One may also be given a modulation function $m(r) \in [0, 1]$, which indicates the degree of certainty of the observation $\hat{\phi}_r$. In probabilistic terms, one may model this situation by considering that the observed phase is obtained from the true (unknown) phase field ϕ with independent observation errors for each pixel, with variance inversely proportional to $m(r)$. Inasmuch as ϕ and $\hat{\phi}$ are angular quantities, an appropriate model for the error probabilities is the Von Mises distribution with inverse variance parameter $m(r)$,[1] so the normalized likelihood of observation $\hat{\phi}_r$ is

$$\hat{p}_r(q) \doteq \mathrm{Probe}(\hat{\phi}_r|\phi_r = q) = \frac{1}{Z}\exp[m(r)\cos(\hat{\phi}_r - q)], \tag{2}$$

where Z is a normalizing constant. Note that, if $m(r) = 0$, $\hat{p}_r$ becomes the uniform distribution, appropriately reflecting the fact that one has complete uncertainty about the true phase value.

To estimate ϕ we propose a strategy in which the probabilistic information contained in the field $\hat{p}$ is smoothed out and propagated from the high certainty regions [where $m(r) \simeq 1$] to the uncertain regions [where $m(r) \simeq 0$]; that is, we propose to compute in a first stage a field of probability distributions $\{p_r, r \in L\}$ that varies smoothly across the lattice—to reflect the fact that the field ϕ should be piecewise smooth—and that is, in some sense, close to the likelihood field $\hat{p}$. Once this p field is computed, one estimates ϕ_r as the value that maximizes the probability $p_r(\phi_r)$ for each site $r \in L$. In fact, the distribution p_r may be interpreted as the posterior marginal probability: $p_r(q) = \Pr(\phi_r = q|\hat{\phi})$ when a prior discrete Markov random field is used to model the field ϕ.[2,3] It can be obtained as the minimizer of the cost function:

$$U(p) = \sum_{r\in L}|p_r - \hat{p}_r|^2 + \lambda\sum_{\langle r,s\rangle}|p_r - p_s|^2, \tag{3}$$

where the second summation ranges over all nearest-neighbor pairs of sites r, s in L and λ is a parameter that controls the smoothness of the p field. Note that, although field p is smooth everywhere, field ϕ may be discontinuous: In the vicinity of a discontinuity of ϕ, the distributions p_r should become strongly bimodal (having peaks at the values of ϕ at both sides of the discontinuity); when one crosses the discontinuity, the global maximum of p_r (and, hence, the optimal estimator ϕ_r) shifts from one peak to the other, producing a jump in the value of ϕ.

In practice, the phase values are discretized into M values $q_1, \ldots, q_M$, with $q_k = 2\pi(k - 1)/(M - 1) - \pi$,

0146-9592/99/241802-03$15.00/0

so p_r and $\hat{p}_r$ become M-vectors and the norm becomes $|f|^2 = \sum_{k=1}^{M} f(k)^2$, where $f(k)$ denotes the kth element of vector f. In this case, Eq. (3) may be written as

$$U(p) = \sum_{k=1}^{M} U_k(p), \quad (4)$$

with

$$U_k(p) = \sum_{r \in L} [p_r(k) - \hat{p}_r(k)]^2 + \lambda \sum_{\langle r,s \rangle} [p_r(k) - p_s(k)]^2.$$

The minimizer of Eq. (4) may be obtained by solution of the M decoupled systems of linear equations that result from equating to zero the partial derivatives of each U_k with respect to the variables $p_r(k)$ for each $r \in L$. Note that it is not necessary to impose explicitly the constraints $\sum_{k=1}^{M} p_r(k) = 1$ and $p_r(k) \geqslant 0$ that make each p_r a valid probability distribution, because it may be proved that the solution automatically satisfies these constraints.[3]

If region L is a rectangle of $n \times m$, where n and m are powers of 2, it is possible to obtain fast approximate solutions by use of the discrete cosine transform (DCT), as explained in Ref. 4. These solutions are of the form

$$p_r(k) = \mathrm{DCT}^{-1}[\rho_k](r), \quad (5)$$

with

$$\rho_k(u,v) = \frac{\mathrm{DCT}[\hat{p}(k)](u,v)}{1 + 2\lambda[2 - \cos(\pi u/m) - \cos(\pi u/m)]},$$

where $\mathrm{DCT}[\hat{p}(k)](u, v)$ denotes the DCT of the field $\{\hat{p}_r(k), r \in L\}$ evaluated at (u, v) and $\mathrm{DCT}^{-1}[\rho_k](r)$ denotes the inverse DCT of ρ_k evaluated at r. Because the DCT implicitly imposes the discrete equivalent of Neumann boundary conditions on the solution, the p field obtained from Eq. (5) will be slightly deformed (with respect to the exact solution) near the borders of the image. In this case, however, this deformation is tolerable, because what matters is not the exact shape of the p field but only which $p_r(k)$ is the largest for each r. If one wants to find the exact solution, or if region L is not a rectangle, one must resort to iterative methods, of which the best choice is possibly the Gauss–Seidel multigrid approach.[5]

In summary, the procedure for estimating the true phase field ϕ, given an observed field $\hat{\phi}$ and a quality function $m(r) \in [0, 1]$, is as follows:

1. Compute normalized likelihood field $\hat{p}_r(q_k)$ for $k = 1, \ldots, M$ and $r \in L$, using Eq. (2), with $q_k = 2\pi(k - 1)/(M - 1) - \pi$.
2. Compute field p, using Eq. (5), for $k = 1, \ldots, M$ and $r \in L$.
3. Find field $\phi_r = q_{k_m(r)}$ for all $r \in L$, where $k_m(r)$ is such that $p_r[k_m(r)] \geqslant p_r(k)$ for all $k \neq k_m(r)$.

To test the algorithm we computed the isoclinic phase map for a diametrically compressed disk. To obtain the photoelastic data we used a circular polariscope in a linear bright-field configuration.[6] The images of Fig. 1 show the lower half of the disk where the point of application of the force is visible in the middle of the bottom part of the disk. Figures 1a and 1b show the terms I_c and I_s, which are computed as[7]

$$I_c(r) = 2m_\alpha(r)\cos[4\alpha(r)] = \frac{I_{\alpha 1}(r) - I_{\alpha 2}(r)}{I_0(r)}, \quad (6)$$

$$I_s(r) = 2m_\alpha(r)\sin[4\alpha(r)] = \frac{2[I_{\alpha 3}(r) - I_0(r)]}{I_0(r)}, \quad (7)$$

where $\alpha(r)$ is the isoclinic parameter to be estimated, $I_{\alpha 1}$, $I_{\alpha 2}$, and $I_{\alpha 3}$ are the images obtained by rotation of the whole polariscope by a series of three angles $\beta_1 = 0$, $\beta_2 = 2\pi/8$, and $\beta_3 = 3\pi/8$, and I_0 is the input intensity, computed as

$$I_0(r) = 1/2\,[I_B(r) + ([I_{\alpha 1}(r) - I_{\alpha 2}(r)]^2 + \{2[I_{\alpha 3}(r) - I_B(r)]\}^2)^{1/2}],$$

with $I_B(r) = 1/2[I_{\alpha 1}(r) + I_{\alpha 2}(r)]$. Modulation m_α, shown in Fig. 1c, is obtained as

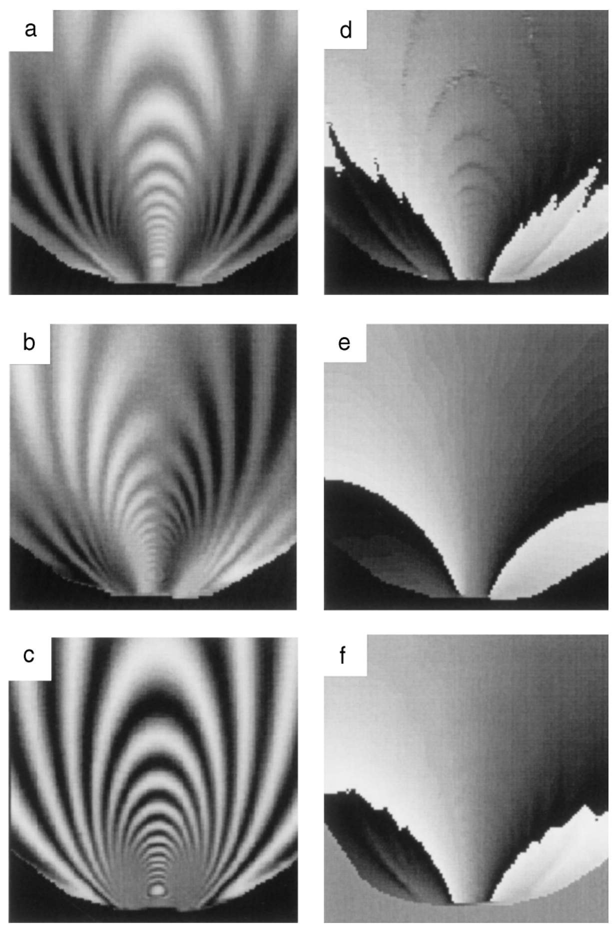

Fig. 1. a, b, I_c and I_s [Eqs. (6) and (7), respectively] for a diamentrically compressed disk. c, Modulation map m_α. d, Observed phase computed as the arctangent of the quotient of b and a. e, Phase reconstructed with the method presented here. f, Phase reconstructed with a conventional interpolation method (see text).

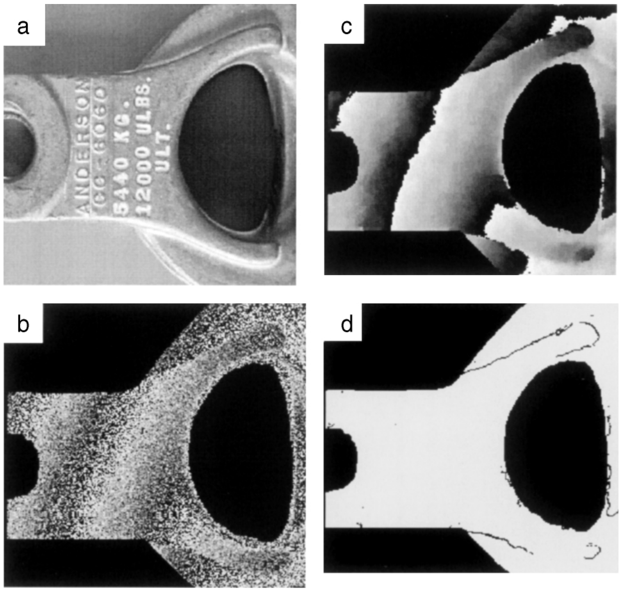

Fig. 2. a, Metallic harness. b, Phase map obtained by temporal phase stepping from four speckle interferograms of a subject to thermal deformation. c, Phase field reconstructed with the method presented here. d, Black pixels indicate phase jumps smaller than 2π.

$$m_\alpha(r) = \frac{([I_{\alpha 1}(r) - I_{\alpha 2}(r)]^2 + \{2[I_{\alpha 3}(r) - I_B(r)]\}^2)^{1/2}}{2I_0(r)} . \tag{8}$$

In this image the dark zones represent low values for the modulation and hence areas where the observed phase is not reliable. Figure 1d shows the observed phase map $\hat{\phi}_r$ as computed from Eq. (1). As one can see, the map appears distorted, particularly close to the low modulation zones. Figure 1e shows the reconstructed phase $\phi = 4\alpha$ obtained by our method. We used $M = 50$ phase levels, $\lambda = 50$, and $m(r) = m_\alpha(r)$ normalized so that it is between 0 and 1; the size of the processed image was 128×128 pixels, and the processing time was $\sim$1.5 s on a machine with a 400-MHz Pentium II processor. Figure 1f shows the reconstructed phase obtained with a conventional interpolation algorithm applied to the sine and the cosine of the observed phase of Fig. 1d, with the points where the modulation map [Eq. (8)] is above a given threshold taken as data for the interpolation.[8] After the interpolation, the phase map is computed as the arctangent of the quotient of the interpolated sine and cosine terms. In this case the threshold value was 0.4 and for the interpolation algorithm we used the griddata function of MatLab.[9] As one can see, the phase map still has some distortions, which are observable in particular close to the phase jumps.

As a second test of the algorithm, we present in Fig. 2 the reconstruction of a discontinuous phase map obtained from four phase-stepping speckle interferograms obtained from the thermal deformation of the mechanical part of Fig. 2a. As one can observe, the method permits effective noise elimination, while both the 2π jumps that are due to the wrapping effected by the arctangent computation and the jumps that are due to the discontinuous nature of the object (shown in Fig. 2d) are adequately preserved. The parameters in this case were $M = 50$ and $\lambda = 20$. The quality map m was set equal to 1 in the region of interest and to 0 outside; in this way, one could still use the fast method based on the DCT, even when the region of interest was not rectangular.

The main drawback of the method is that it implies the solution of M decoupled linear systems of equations, where M is the number of quantization levels of the reconstructed phase. If high precision—and, hence, a large value of M—is desired, this may imply a relatively high computational cost in both time and memory requirements. For example, for a 256×256 image with $M = 128$, the processing time is $\sim$55 s on a 400-MHz Pentium II machine, and the memory requirement is $\sim$70 Mbytes. In view of modern computational capabilities, however, these requirements do not seem excessive.

The authors thank M. Rivera for many useful discussions. J. L. Marroquín and R. Rodriguez-Vera were supported in part by grants from the Consejo Nacional de Ciencia y Tecnología, Mexico. J. A. Quiroga was supported by a postdoctoral grant from the Universidad Complutense de Madrid and by the "Becas Internacionales Flores-Valles" program, Spain. We are thankful for the support of the Centro de Investigaciones en Óptica León, Mexico. J. L. Marroquin's e-mail address is jlm@fractal.cimat.mx.

References

1. N. I. Fisher, *Statistical Analysis of Circular Data* (Cambridge U. Press, Cambridge, 1993).
2. J. L. Marroquin, M. Rivera, and S. Botello, Proc. SPIE **3459,** 238 (1998).
3. J. L. Marroquin, R. Rodriquez-Vera, and M. Servin, J. Opt. Soc. Am. A **15,** 6 (1998).
4. D. C. Ghiglia and L. A. Romero, J. Opt. Soc. Am. A **11,** 107 (1994).
5. S. Botello, J. L. Marroquin, and M. Rivera, Appl. Opt. **37,** 7587 (1998).
6. P. S. Theocaris and E. E. Gdoutos, *Matrix Methods in Photoelasticity* (Springer-Verlag, Berlin, 1979).
7. J. A. Quiroga and A. Gonzalez-Cano, Proc. SPIE **3744,** 328 (1999).
8. N. Plouzennec, J. C. Dupré, and A. Lagarde, Exp. Tech. **23**(1), 30 (1999).
9. MathWorks, "Matlab function reference," on-line version (MathWorks, Inc., 1998; http://www.mathworks.com).